

## REVIEW

Cite this: *Chem. Sci.*, 2021, 12, 540Received 17th September 2020  
Accepted 20th November 2020

DOI: 10.1039/d0sc05148a

rsc.li/chemical-science

# Determination and perturbation of the electronic potentials of solid catalysts for innovative catalysis

Xingyu Qi,  Tatsuya Shinagawa,  Fuminao Kishimoto and Kazuhiro Takanabe \*

Concerns about energy and the environment are motivating a reexamination of catalytic processes, aiming to achieve more efficient and improved catalysis compatible with sustainability. Designing an active site for such heterogeneous catalytic processes remains a challenge leading to a next level breakthrough. Herein, we discuss a fundamental aspect of heterogeneous catalysis: the chemical potential of electrons in solid catalysts during thermal catalysis, which directly reflects the consequent catalytic reaction rate. The use of electrochemical tools during thermal catalysis allows for the quantitative determination of the ill-defined chemical potentials of solids *in operando*, whereby the potential–rate relationship can be established. Furthermore, the electrochemical means can also introduce the direct perturbation of catalyst potentials, in turn, perturbing the coverage of adsorbates functioning as poison, promoters, or reactants. We collect selected publications on these aspects, and provide a viewpoint bridging the fields of thermal- and electro-catalysis.

## Introduction

For centuries, our society has relied on catalytic processes in industry.<sup>1,2</sup> Historically, economic growth had been the primary concern, linked with the large production of commodity chemicals, which is, however, required to balance with its impact on the environment.<sup>3</sup> Building upon the fundamental understanding of catalysis hitherto established, it is imperative to revisit catalytic systems, to achieve more efficient catalytic systems and more advanced characterization. Determination of the electronic state or Fermi level of the catalyst, especially during catalysis, is one of the key factors to scale its performance.<sup>4–5</sup> On this basis, we envisage that the determination and active perturbation of the catalyst potential can pave the way for sustainable alternatives.

The past few decades have witnessed much research activity on determining the electronic state of a substance as well as its chemical manipulation by the addition of a foreign component.<sup>6–8</sup> In the field of surface science, for instance, Kiskinova *et al.* experimentally measured the work function (WF) of Pt(111) under vacuum to be 5.9 eV by using ultra-violet photo-emission spectroscopy.<sup>9</sup> These authors observed that the addition of potassium at a coverage of 0.17 on Pt(111) changed its WF to 1.3 eV, resulting in an increased electron back donation to the  $2\pi^*$  orbital of chemisorbed CO with stronger Pt–C and weaker C–O bonds.<sup>9</sup> Another representative study using a Kelvin probe force microscope examined WF at the surface of Au

nanoparticles deposited on an n-doped Si substrate and found that the WF of nano-sized Au decreased when in contact with n-Si, indicative of electron transfer from n-Si to Au.<sup>10</sup> Additionally, the electronic and molecular structures of the solid–liquid interface also attract attention, which is considered as key to the development of catalytic reactions.<sup>11</sup> In 2009, the group of Domen demonstrated the direct probing of the Fermi level of Pt metal nanoparticles on a GaN wafer in water under ultraviolet irradiation using the application of *in situ* attenuated total reflection surface-enhanced infrared absorption spectroscopy (ATR-SEIRAS).<sup>12</sup> By correlating the vibrational frequency of probe molecules (CO) on Pt with the electrochemical applied potential, the potential shift of Pt on a self-standing Pt/GaN photocatalyst under light illumination was estimated by following the CO vibrational frequency, which shows a good example of revealing the electronic states of catalysts involved at the solid–liquid interfaces.<sup>12</sup> Notably, the recent development of computational tools corroborated these experimental studies.<sup>5</sup> The group of Nørskov theoretically studied the electronic structure and reactivity trends of transition and noble metal surfaces by performing density functional theory (DFT) calculations.<sup>13</sup> Particularly, they addressed the centre of the d-bands of metals that reflects the interaction between metal electrons and an unoccupied state of the adsorbate, such as  $2\pi^*$  for chemisorbed CO, and computationally demonstrated that the coupling between these orbitals, to a large extent, determines the chemisorption energy.<sup>13</sup>

By applying this fundamental understanding, we can detail the so-called “metal–support interaction” (MSI) and “promoter effect” in the field of catalysis.<sup>14–17</sup> When an active metal particle is supported on some oxides, such as SrTiO<sub>3</sub> (ref. 14) and

Department of Chemical System Engineering, School of Engineering, The University of Tokyo, 7-3-1 Hongo, Bunkyo-ku, Tokyo, Japan. E-mail: takanabe@chemsys.t.u-tokyo.ac.jp



CeO<sub>2</sub>,<sup>17</sup> with a distinct Fermi level or physically in contact with elements having a lower WF, such as alkali,<sup>16</sup> alkali-earth,<sup>18</sup> or rare-earth<sup>18</sup> elements, it exhibited facile dissociative adsorption of reactants, such as N<sub>2</sub>, and thus a higher reaction rate.<sup>16,17</sup> We can account for the rate enhancement by the electron transfer between the substances, whereby the catalyst attains an electrochemical potential distinct from its pristine state. A recent study “counting” the number of electrons transferred between the Pt catalyst and CeO<sub>2</sub>(111) support by resonant photoemission spectroscopy and X-ray photoelectron spectroscopy (XPS) further validated the quantitative description of the Fermi level of the supported metal catalysts.<sup>19</sup> Advances in synchrotron radiation XPS and electrochemical infrared spectroscopy also helped observe the change of the electronic state of the metal at the interface with oxide supports.<sup>20</sup> The consequence of the change in the catalyst potential is the alteration of its binding strength to the surface adsorbate<sup>21,22</sup> and thereby the reaction rate.

From a different perspective, in the field of electrochemistry, the electric potential is the primary parameter to control the rate of electrode reactions, measured as current.<sup>23</sup> By applying more positive [negative] potentials, anodic [cathodic] reaction rates kinetically increase.<sup>24,25</sup> More precisely, the application of external bias causes the chemical potential of the reactants and products of the electrode reaction to deviate from their original equilibrium state.<sup>26</sup> Consequently, the activation energy of the reaction changes, resulting in the alteration of the reaction rate, as evidenced both experimentally<sup>27</sup> and computationally.<sup>28</sup>

These studies provide insights into how the electrochemical potential plays a decisive role in the reactivity of metal catalysts. However, these surface science techniques require either demanding experimental conditions<sup>19</sup> or advanced equipment,<sup>20</sup> which cannot universally reveal the catalyst potential during the reaction *in operando*. In what follows, by bridging the fields of thermal- and electro-catalysis, we elaborate the correlation between the potential of a thermal catalyst and its catalytic performance in an electrochemical manner, quantitatively detailing the fundamental aspects of catalytic reactions,<sup>29,30</sup> and review studies on the *in operando* determination of the catalyst potential using electrochemical tools. Subsequently, we discuss the perturbation of the catalyst potential using electrochemical tools that induce the generation of the promoter, removal of poison, perturbation of intermediate-coverage on the surface, and local alteration of the vicinity of active sites, as illustrated in Fig. 1, aiming at providing a refined view into the electrochemical promotion of thermal catalytic reactions.

## Electrochemical potential determination of a solid catalyst during thermal catalytic reactions

To quantitatively measure the potential of solids *in operando*, the material of interest can be fabricated into a working electrode (WE) in contact with an adequate electrolyte environment. Using a three-electrode setup, the WE potential is scaled relative to a reference electrode (RE) even under open-circuit

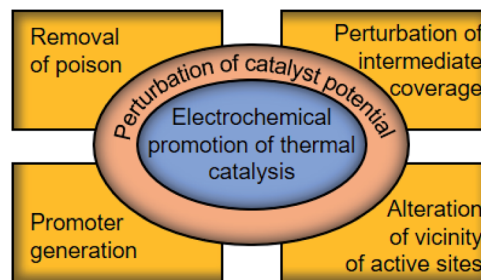


Fig. 1 Electrochemical promotion of thermal-catalysis can be achieved by perturbing the catalyst potential with electrochemical tools, which induces promoter generation, perturbation of intermediate-coverage, and removal of poison, as well as alteration of the vicinity of active sites.

conditions, *i.e.*, no current flow,<sup>31</sup> which directly corresponds to the Fermi level of the WE. With concurrent detection of substances produced by thermal catalysis as a measure of the reaction rate, the potential–performance correlation can be established.<sup>32,33</sup> Obviously, the limitation of this application is only for materials to be conductive enough to achieve electronic circuits. The employed electrochemical setup therein does not necessarily require well-defined clean systems such as single crystals, and thus would be tolerant to some impurities to the same extent as industrialized electrochemical processes.

The Marin group<sup>33</sup> measured the (thermal) oxidation rate of methyl  $\alpha$ -D-glucopyranoside with O<sub>2</sub> catalysed by 3.3 wt% Pt/graphite, while monitoring the catalyst potential *in operando*. These authors observed a continuous shift of the open-circuit potential (OCP) with time to a more positive potential as the reaction rate decreased. The oxidation rate decreased from 2.5 mmol kg<sub>cat</sub><sup>-1</sup> s<sup>-1</sup> to the steady-state value of 0.5 mmol kg<sub>cat</sub><sup>-1</sup> s<sup>-1</sup>, which coincided with the OCP shift from 0.4 V *vs.* the reversible hydrogen electrode (RHE) to, finally, 0.9 V *vs.* RHE.<sup>33</sup> The Marin group proposed that upon exposure to the O<sub>2</sub> reactant, the OCP changed due to an increase in the O<sub>ad</sub> coverage, followed by the gradual formation of inactive O in the sublayer to reach a more positive potential, and further built a Langmuir–Hinshelwood type of kinetic model to describe the reaction over a board range of conditions.<sup>33</sup> In 2014, Tao *et al.*<sup>4</sup> corroborated this view by quantitatively determining the surface adsorbate by infrared spectroscopy while measuring the OCP and the reaction rate for the reaction between CO and pre-oxidized Pt. These studies demonstrate the measurements of the potential during catalysis as a powerful tool to rationalize the surface state, which in turn dictates the catalytic performance.

Such determination of the electronic potential of the catalyst in the working state can also be a powerful tool to elucidate the reaction mechanism. In one example, according to the mixed potential theory,<sup>34,35</sup> each catalyst particle functions as a short-circuit electrochemical cell, where both electrochemical half-reactions, *i.e.*, reduction and oxidation reactions, occur at the same rate, leading to the unified potential. By analysing the overall rate and each half-reaction rate, controversial

mechanisms can be elucidated whether there is internal faradaic charge transfer or not in a thermal-catalytic reaction.

## Approaches to alter the potential of a solid catalyst for heterogeneous reactions

We now discuss active perturbation of the solid potential by applying an electrochemical setup to alter the thermal-catalytic reaction rate in a distinct manner from the electrocatalytic process. Such electrochemical promotion of the catalyst changes the reaction rate and is therefore only applicable to steady-state reactions with  $\Delta G < 0$  at a given reaction temperature, which contrasts with electrocatalytic processes.<sup>26,36</sup> In electrocatalysis, electric power acts as energy input to polarize the electrode potential beyond the equilibrium potential, thereby making the reaction thermodynamically allowed to proceed.<sup>26</sup> The electrochemical promotion of the active sites can directly alter the structure of the activated complex at the transition state, or influence the coverage of species on the surface that function as a promoter, reaction intermediate, or poison. The following are some examples of the promotion effects of thermal catalysis.

The group of Vayenas<sup>37,38</sup> reported the pioneering work of promoted catalysis induced by altering the potential with electrochemical tools, and named it non-faradaic electrochemical modification of catalytic activity (NEMCA) or electrochemical promotion of catalysis (EPOC). As shown in Fig. 2a, their system is composed of a solid electrolyte, whose one side is decorated with the catalyst film prepared with commercial metal paste

and functions as a WE, while the other side plays the role of a counter electrode (CE). By externally applying a voltage between the WE and CE, the promoted catalytic rate consisting of the rate at the OCP ( $r_{\text{OCP}}$ ), faradaic rate ( $r_f$ ), and extra rate of promotion ( $r_p$ ) can be observed, as illustrated in Fig. 2b. The mechanism accounting for such improvement is that the charge carriers in the solid electrolyte “spill-over” the surface of the supported catalyst and the spilled-over species alters the WF of the catalyst, and thereby functions as a promoter, as schematically illustrated in Fig. 2c.<sup>36</sup> Such a change in the WF alters the activation energy of the reaction, resulting in improved thermal-catalytic performance in a reversible manner compared to that without the applied voltage.<sup>39–42</sup> As one example, the hydrogenation of  $\text{CO}_2$  over Ru deposited on a proton-conducting oxide ( $\text{BaZr}_{0.85}\text{Y}_{0.15}\text{O}_{3-\alpha}$  + 1 wt% NiO) has been investigated.<sup>41,43</sup> Their study showed that positively polarizing the WF removed the proton promoter and, in turn, enhanced thermal-catalytic  $\text{CH}_4$  formation and suppressed the CO formation rate, while negatively polarizing the WF resulted in an opposite manner.<sup>41,43</sup> A similar promotion effect was also observed in a liquid phase for the  $\text{H}_2 + \text{O}_2$  reaction, demonstrating the applicability of NEMCA to various reactions.<sup>44–47</sup>

In a distinct mechanism, externally applying electric potentials onto the catalyst tunes its WF as in the electrochemical process, and facilitates the formation or consumption of the surface adsorbate that is otherwise considerably slow in the thermal-catalytic manner.<sup>48–51</sup> More specifically, a change in the WF of the solid catalyst leads to subsequent alteration of its binding energy to surface species, and thereby the adsorption energy is changed. According to the Brønsted–Evans–Polanyi relationship, the activation energy  $E_a$  linearly scales with the adsorption energy  $\Delta E$ :<sup>52</sup>

$$E_a = \alpha \Delta E + \beta \quad (1)$$

which indicates that the change in the adsorption energy will result in the corresponding change of the activation energy and thereby of the reaction rate. The group of Strasser<sup>48</sup> observed that the chemical decomposition of  $\text{N}_2\text{H}_4$  was promoted when a potential of 0.1 V vs. RHE was applied over a Ni–Co alloy with respect to the open-circuit condition. These authors attributed the enhancement to the accelerated formation of  $\text{N}_2\text{H}_{4\text{ad}}$  on the catalyst surface at the positive potential, which is the “shared” intermediate for both electrochemical and electroless pathways, as shown in Fig. 3a.<sup>48</sup> Similarly promoted adsorption of a reaction intermediate was reported for the hydrogenation of maleic acid, in which the applied potential facilitated the dissociative adsorption and increased the mobility of active  $\text{H}_{\text{ad}}$ .<sup>50</sup>

From a more general perspective, the direct application of potential can tune the coverage of adsorbed species on the surfaces. More precisely, by pinning the potential of solids during the thermal-catalytic reaction with an electrochemical means, we can control the surface state of a solid, e.g., to keep the surface clean from passivation or poisoning. This interesting approach was reported in 2018 by the group of Lercher for the hydrogenation of benzaldehyde over a Ni catalyst.<sup>49</sup> The Ni surface was inert for hydrogenation of benzaldehyde at the

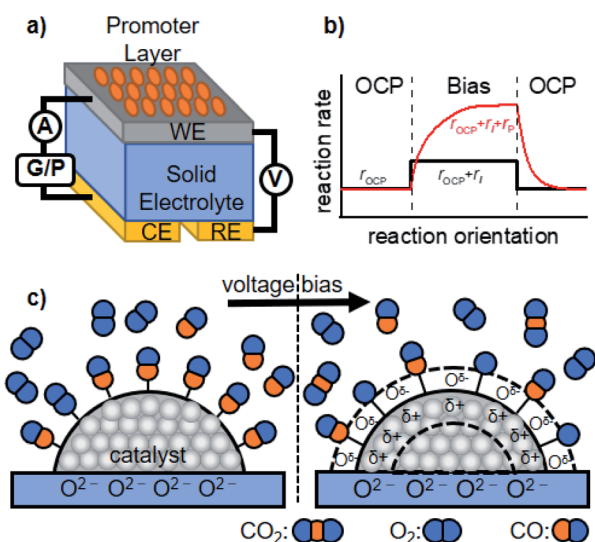


Fig. 2 Schematic representation of the (a) basic experimental setup for NEMCA, (b) typical transient NEMCA curve showing the reaction rate at the OCP ( $r_{\text{OCP}}$ ), faradaic reaction rate ( $r_f$ ) and extra rate of promotion ( $r_p$ ) caused by bias application, and (c) spilling-over of the promoter on the surface of the supported catalyst induced by external voltage bias and its consequent change of adsorption of reactants using CO oxidation as an example. The figure was drawn based on ref. 36.

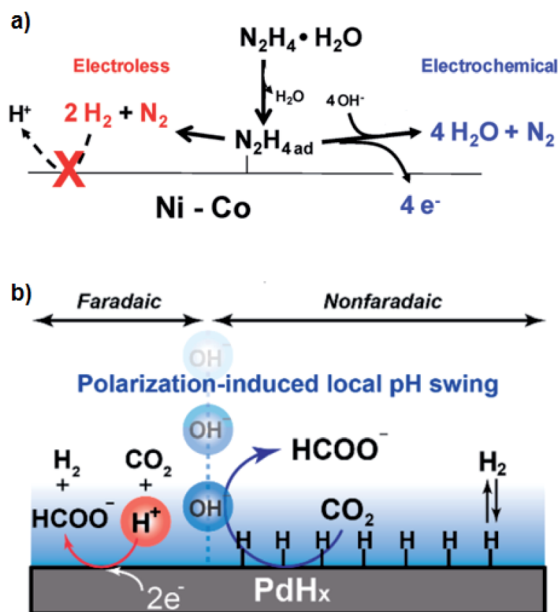


Fig. 3 Mechanism of (a) electrochemically promoted formation of  $N_2H_{4ad}$  that acts as the shared intermediate for both electro- and thermal-pathways<sup>48</sup> and (b) improved thermal catalysis of  $CO_2$  hydrogenation by polarization-induced local pH swing.<sup>53</sup> Reprinted (adapted) with permission from ref. 48 and 53. Copyright 2011 American Chemical Society. Copyright 2020 American Chemical Society.

OCP due to the strong binding of  $O_{ad}$  species on the surface, which, however, became active upon the application of a potential negative enough to reduce Ni–O species.<sup>49</sup>

The electrochemical promotion system in the liquid phase might additionally benefit from the “polarization-induced local pH swing”.<sup>53</sup> Ryu *et al.*<sup>53</sup> observed that the hydrogenation rate of  $CO_2$  over a Pd catalyst in the aqueous phase was positively correlated with the alkalinity of the reaction media. Building on the correlation, they cathodically polarized the system to induce local alkaline environments in an electrochemical manner.<sup>53</sup> Consequently, as schematically illustrated in Fig. 3b, this electrochemical perturbation resulted in the promotion of the thermal-catalytic  $CO_2$  hydrogenation reaction.<sup>53</sup>

The electrochemical promotion, in principle, can be achieved for all steady-state reactions with  $\Delta G < 0$ , and should only have kinetic effects unless a substantial external current is applied. Electronic consequences caused by classical promotion (*e.g.*, promoters and MSI) are, after all, similar phenomena to the EPOC, which is however driven by different devices.<sup>36,46</sup> Compared to conventional promotion, electrochemical promotion can manipulate the potential of the solid catalyst more precisely by utilizing external electrochemical devices. However, targeted electrochemical promotion effects can only be realized when certain sufficient criteria are met. Firstly, the system must achieve a delicate balance that allows the back-spillover of the promoter to be faster than its desorption or consumption, *i.e.*, slow kinetics of promoter destruction.<sup>36,54</sup> By appropriate catalyst–electrode design as well as appropriate choice of electrolyte that can maintain the effective promoter

layer, the above criterion can be met,<sup>36</sup> and investigations on better combinations for targeted chemical reactions can be one of the directions for the research of this aspect. Secondly, it is important to control the contribution of the non-faradaic reaction relative to that of the faradaic one when the EPOC is operational.<sup>36</sup> Maximizing the apparent electrochemical promotion effect thus requires optimizing not only the catalyst materials but also reaction conditions, *e.g.*, applied external potentials. Another challenging issue for gas reactions performed in a liquid system is the slow diffusion of gas reactants caused by low solubility, which limits the total reaction rate in practical applications. Such a mass-transport limitation can be mitigated by the use of membrane–electrode assembly, which allows the direct supply of gas reactants to the catalyst surfaces without diffusion limitations. Designing better experimental setups for more pronounced promotion effects is surely another target that researchers are going to pay attention to.

Lastly, we address how to quantify the active sites of the targeted reactions, which might be one of the major concerns of researchers. In some electrochemical promotion systems, the number of active sites would remain unchanged when the external potential/current is applied, since the application of electric field basically induces the supply of a promoter without restructuring the catalyst surface. This type of simple system allows for quantification of the active sites by the conventional means such as the chemisorption and desorption of appropriate probe molecules *ex situ* under unpromoted conditions.<sup>55</sup> However, in some other systems where the reconstruction of the catalyst and/or the removal of poisoning occurs when the external potential/current is applied, and the number of active sites changes, the quantification requires the employment of sophisticated *in situ* or *operando* characterization, for instance, stripping of adsorbed probe species<sup>56</sup> or infrared spectroscopy.<sup>57</sup>

## Outlook for other innovative catalysis

From the viewpoint of electrochemically promoting thermal-catalytic reactions, one novel approach has been reported by the group of Sekine.<sup>58,59</sup> These authors applied voltage to the particulate catalyst of 9.9 wt% Cs/5.0 wt% Ru/SrZrO<sub>3</sub> for ammonia synthesis, distinct from the disk-shaped electrode employed for the NEMCA.<sup>58</sup> Its consequence was also the lowered activation energy of reaction and improved catalytic rates, accompanying a change in the reaction mechanism from dissociative to associative.<sup>58</sup> The origin of this improvement remains elusive. However, the reaction path mediated by the surface proton is proposed as the plausible one.<sup>58</sup> In addition, the applied voltage would form an electric field in the vicinity of the surfaces, which itself also impacts the catalysis.<sup>60</sup> Interested readers are referred to the recent report by the group of Sekine.<sup>59</sup> In another example, a DFT study by Jafarzadeh *et al.* found that Cu favors physisorption of  $CO_2$ , which, when placed in an electric field, switches to chemisorption by bending  $CO_2$  molecules.<sup>61</sup>

Lastly, based on the understanding of the decisive role of the potential in catalysis, we can now revisit the “MSI” for innovative catalysis. Upon light illumination, the photon-induced

charge transfer of the excited carriers between the metal particle and semiconductor support can provide a steady-state potential shift of the active surfaces, resulting in different thermal catalytic reactivity.<sup>62</sup> For instance, choosing n- or p-type semiconductors as the support can determine the type of contact, either Schottky or ohmic, which additionally dictate the charge transfer at the interface.<sup>63</sup> Using Pt supported on p- or n-GaN as a model, the groups of Lercher and Stutzmann studied the variation in the electronic structure of Pt.<sup>64</sup> Its resultant catalysis was also altered; higher activity for thermal CO oxidation over Pt/n-GaN than over Pt/p-GaN was observed.<sup>62</sup> The electronegative is another non-conventional support, where, according to the research of Hosono's group, by the electron donation from the support to the metal, the catalyst can not only lower the activation energy of ammonia synthesis over a Ru catalyst, but also suppress the poisoning of the Ru surface caused by H adatoms.<sup>65</sup> The application of such novel materials to the support would open a new frontier of supported metal catalysis.

## Summary

In this minireview, we highlighted how the catalyst potential plays a decisive role in catalytic reactions. First, we reviewed the determination of the catalyst potential with various experimental tools while concurrently measuring the reaction rate, which allows for quantitatively establishing the potential–rate relationship. Next, we showed that the active perturbation of the potential by electrochemical methods alters the catalyst WF and thereby the surface coverage of the adsorbate that functions as a promoter, poison, or reactant. Toward the end, we shared other examples that utilize an electric field or non-conventional catalyst–support, adding another viewpoint to the promoted thermal-catalytic reactions. Herein we provide a view bridging the field of thermal- and electro-catalysis, paving the way for innovative catalysis.

## Conflicts of interest

There are no conflicts to declare.

## Acknowledgements

This work was supported by JSPS KAKENHI Grant Number 19H02510 and 20K15084.

## References

- 1 S. L. Foster, S. I. P. Bakovic, R. D. Duda, S. Maheshwari, R. D. Milton, S. D. Minter, M. J. Janik, J. N. Renner and L. F. Greenlee, *Nat. Catal.*, 2018, **1**, 490–500.
- 2 J. Sun and Y. Wang, *ACS Catal.*, 2014, **4**, 1078–1090.
- 3 K.-i. Shimizu and A. Satsuma, *Energy Environ. Sci.*, 2011, **4**, 3140–3153.
- 4 Q. Tao, Y.-L. Zheng, D.-C. Jiang, Y.-X. Chen, Z. Jusys and R. J. Behm, *J. Phys. Chem. C*, 2014, **118**, 6799–6808.
- 5 J. Greeley, J. K. Nørskov and M. Mavrikakis, *Annu. Rev. Phys. Chem.*, 2002, **53**, 319–348.
- 6 D. C. Koningsberger, J. de Graaf, B. L. Mojet, D. E. Ramaker and J. T. Miller, *Appl. Catal., A*, 2000, **191**, 205–220.
- 7 P. Li, X. Duan, Y. Kuang, Y. Li, G. Zhang, W. Liu and X. Sun, *Adv. Energy Mater.*, 2018, **8**, 1703341.
- 8 J. L. Gland and G. A. Somorjai, *Surf. Sci.*, 1973, **38**, 157–186.
- 9 M. Kiskinova, G. Pirug and H. P. Bonzel, *Surf. Sci.*, 1983, **133**, 321–343.
- 10 Y. Zhang, O. Pluchery, L. Caillard, A.-F. Lamic-Humblot, S. Casale, Y. J. Chabal and M. Salmeron, *Nano Lett.*, 2015, **15**, 51–55.
- 11 F. Zaera, *Chem. Rev.*, 2012, **112**, 2920–2986.
- 12 M. Yoshida, A. Yamakata, K. Takanebe, J. Kubota, M. Osawa and K. Domen, *J. Am. Chem. Soc.*, 2009, **131**, 13218–13219.
- 13 A. Ruban, B. Hammer, P. Stoltze, H. L. Skriver and J. K. Nørskov, *J. Mol. Catal. A: Chem.*, 1997, **115**, 421–429.
- 14 M. Qureshi, A. T. Garcia-Esparza, G. Jeantelot, S. Ould-Chikh, A. Aguilar-Tapia, J.-L. Hazemann, J.-M. Basset, D. Loffreda, T. Le Bahers and K. Takanebe, *J. Catal.*, 2019, **376**, 180–190.
- 15 T. W. van Deelen, C. Hernández Mejía and K. P. de Jong, *Nat. Catal.*, 2019, **2**, 955–970.
- 16 K. Aika, A. Ohya, A. Ozaki, Y. Inoue and I. Yasumori, *J. Catal.*, 1985, **92**, 305–311.
- 17 A. Bruix, J. A. Rodriguez, P. J. Ramirez, S. D. Senanayake, J. Evans, J. B. Park, D. Stacchiola, P. Liu, J. Hrbek and F. Illas, *J. Am. Chem. Soc.*, 2012, **134**, 8968–8974.
- 18 K.-i. Aika, T. Takano and S. Murata, *J. Catal.*, 1992, **136**, 126–140.
- 19 Y. Lykhach, S. M. Kozlov, T. Skála, A. Tovt, V. Stetsovych, N. Tsud, F. Dvořák, V. Johánek, A. Neitzel, J. Mysliveček, S. Fabris, V. Matolín, K. M. Neyman and J. Libuda, *Nat. Mater.*, 2016, **15**, 284–288.
- 20 F. Faisal, C. Stumm, M. Bertram, F. Waidhas, Y. Lykhach, S. Cherevko, F. Xiang, M. Ammon, M. Vorokhta and B. Šmíd, *Nat. Mater.*, 2018, **17**, 592–598.
- 21 S. A. Wasileski, M. J. Weaver and M. T. M. Koper, *J. Electroanal. Chem.*, 2001, **500**, 344–355.
- 22 S. A. Wasileski, M. T. M. Koper and M. J. Weaver, *J. Chem. Phys.*, 2001, **115**, 8193–8203.
- 23 M. Tsionsky, A. J. Bard and M. V. Mirkin, *J. Phys. Chem.*, 1996, **100**, 17881–17888.
- 24 M. Navarro, W. F. De Giovanni and J. R. Romero, *J. Mol. Catal. A: Chem.*, 1998, **135**, 249–256.
- 25 A. Funakawa, I. Yamanaka, S. Takenaka and K. Otsuka, *J. Am. Chem. Soc.*, 2004, **126**, 5346–5347.
- 26 A. J. Bard and L. R. Faulkner, *Electrochemical Methods: Fundamentals and Applications*, John Wiley & Sons, Inc., New York, 2nd edn, 2001.
- 27 V. S. Protsenko and F. I. Danilov, *J. Electroanal. Chem.*, 2011, **651**, 105–110.
- 28 A. B. Anderson and T. V. Albu, *Electrochem. Commun.*, 1999, **1**, 203–206.
- 29 Y. Wei, K. F. Hsueh and G.-W. Jang, *Polymer*, 1994, **35**, 3572–3575.
- 30 G. Horanyi, *Catal. Today*, 1994, **19**, 285–311.
- 31 J. A. S. Roberts and R. M. Bullock, *Inorg. Chem.*, 2013, **52**, 3823–3835.

- 32 L. Jelemensky, B. F. M. Kuster and G. B. Marin, *Ind. Eng. Chem. Res.*, 1997, **36**, 3065–3074.
- 33 J. H. Vleeming, B. F. M. Kuster and G. B. Marin, *Ind. Eng. Chem. Res.*, 1997, **36**, 3541–3553.
- 34 T. Mallat and A. Baiker, *Catal. Today*, 1995, **24**, 143–150.
- 35 A. Mills, *Chem. Soc. Rev.*, 1989, **18**, 285–316.
- 36 C. G. Vayenas, S. Bebelis, C. Pliangos, S. Brosda and D. Tsiplakides, *Electrochemical activation of catalysis: promotion, electrochemical promotion, and metal-support interactions*, Springer Science & Business Media, 2001.
- 37 M. Stoukides and C. G. Vayenas, *J. Catal.*, 1981, **70**, 137–146.
- 38 A. Katsaounis, *J. Appl. Electrochem.*, 2010, **40**, 885–902.
- 39 A. de Lucas-Consuegra, J. González-Cobos, Y. García-Rodríguez, A. Mosquera, J. L. Endrino and J. L. Valverde, *J. Catal.*, 2012, **293**, 149–157.
- 40 I. Kalaitzidou, M. Makri, D. Theleritis, A. Katsaounis and C. G. Vayenas, *Surf. Sci.*, 2016, **646**, 194–203.
- 41 A. Kotsiras, I. Kalaitzidou, D. Grigoriou, A. Symillidis, M. Makri, A. Katsaounis and C. G. Vayenas, *Appl. Catal., B*, 2018, **232**, 60–68.
- 42 D. Poulidi and I. S. Metcalfe, *Chem. Eng. Sci.*, 2010, **65**, 446–450.
- 43 I. Kalaitzidou, A. Katsaounis, T. Norby and C. G. Vayenas, *J. Catal.*, 2015, **331**, 98–109.
- 44 S. G. Neophytides, D. Tsiplakides, P. Stonehart, M. M. Jaksic and C. G. Vayenas, *Nature*, 1994, **370**, 45–47.
- 45 S. G. Neophytides, D. Tsiplakides, P. Stonehart, M. Jaksic and C. G. Vayenas, *J. Phys. Chem.*, 1996, **100**, 14803–14814.
- 46 D. Labou and S. G. Neophytides, *Top. Catal.*, 2007, **44**, 451–460.
- 47 E. Ruiz-López, A. Caravaca, P. Vernoux, F. Dorado and A. de Lucas-Consuegra, *Chem. Eng. J.*, 2020, **396**, 125217.
- 48 J. Sanabria-Chinchilla, K. Asazawa, T. Sakamoto, K. Yamada, H. Tanaka and P. Strasser, *J. Am. Chem. Soc.*, 2011, **133**, 5425–5431.
- 49 Y. Song, U. Sanyal, D. Pangotra, J. D. Holladay, D. M. Camaioni, O. Y. Gutiérrez and J. A. Lercher, *J. Catal.*, 2018, **359**, 68–75.
- 50 E. Lamy-Pitara, S. El Mouahid and J. Barbier, *Electrochim. Acta*, 2000, **45**, 4299–4308.
- 51 F. Cai, D. Gao, H. Zhou, G. Wang, T. He, H. Gong, S. Miao, F. Yang, J. Wang and X. Bao, *Chem. Sci.*, 2017, **8**, 2569–2573.
- 52 T. Bliigaard, J. K. Nørskov, S. Dahl, J. Matthiesen, C. H. Christensen and J. Sehested, *J. Catal.*, 2004, **224**, 206–217.
- 53 J. Ryu and Y. Surendranath, *J. Am. Chem. Soc.*, 2020, **142**, 13384–13390.
- 54 S. Brosda, C. G. Vayenas and J. Wei, *Appl. Catal., B*, 2006, **68**, 109–124.
- 55 L. J. Burcham, L. E. Briand and I. E. Wachs, *Langmuir*, 2001, **17**, 6164–6174.
- 56 D. Malko, A. Kucernak and T. Lopes, *Nat. Commun.*, 2016, **7**, 1–7.
- 57 C. M. Gunathunge, J. Li, X. Li and M. M. Waegle, *ACS Catal.*, 2020, **10**, 11700–11711.
- 58 R. Manabe, H. Nakatsubo, A. Gondo, K. Murakami, S. Ogo, H. Tsuneki, M. Ikeda, A. Ishikawa, H. Nakai and Y. Sekine, *Chem. Sci.*, 2017, **8**, 5434–5439.
- 59 Y. Sekine and R. Manabe, *Faraday Discuss.*, 2020, DOI: 10.1039/C9FD00129H.
- 60 F. Che, J. T. Gray, S. Ha, N. Kruse, S. L. Scott and J.-S. McEwen, *ACS Catal.*, 2018, **8**, 5153–5174.
- 61 A. Jafarzadeh, K. M. Bal, A. Bogaerts and E. C. Neyts, *J. Phys. Chem. C*, 2020, **124**, 6747–6755.
- 62 S. M. Kim, D. Park, Y. Yuk, S. H. Kim and J. Y. Park, *Faraday Discuss.*, 2013, **162**, 355–364.
- 63 H. Zhong, Z. Liu, G. Xu, Y. Fan, J. Wang, X. Zhang, L. Liu, K. Xu and H. Yang, *Appl. Phys. Lett.*, 2012, **100**, 122108.
- 64 S. Schäfer, S. A. Wyrzgol, R. Caterino, A. Jentys, S. J. Schoell, M. Hävecker, A. Knop-Gericke, J. A. Lercher, I. D. Sharp and M. Stutzmann, *J. Am. Chem. Soc.*, 2012, **134**, 12528–12535.
- 65 M. Kitano, Y. Inoue, Y. Yamazaki, F. Hayashi, S. Kanbara, S. Matsuiishi, T. Yokoyama, S.-W. Kim, M. Hara and H. Hosono, *Nat. Chem.*, 2012, **4**, 934–940.